Free-Surface Effects on the Advancing 3-D Slender Body

Shiann-Jorng Horng, Shean-Kwang Chou,

Ching-Tarng Liaw and Jin-Der Jiang

Institute of Harbor & Marine Technology

Wuchi, Taiwan, R.O.C.

Sponsored by

The National Science Council

Under Grant NSC82-0209-E-124-006

Table of Contents

List of Figures

ABSTRACT

This paper applies the boundary element method to solve the fluid-structure interaction problems during heaving and pitching motions with speed of a wigley and Series 60 ship model. The 3-D fluid motion in the infinite region is approximated by the unsteady 2-D flow in the finite region with an artificial open boundary on which a more relaxed Sommerfeld's radiation condition is imposed. The heave and pitch diagonal and off-diagonal added mass and damping coefficients of a Wigley and Series 60 ship model calculated by the present method are compared well and have the same trend as the experimental and other authors' results. The present method is a very good method for the calculation of the heave and pitch diagonal and off-diagonal added mass and damping coefficients of Wigley model and Series 60 ship model moving with speed.

摘　要

本文以邊界元素法求解一數學船及一Series 60船型前進且附帶有簡諧性上下搖及縱搖運動時之流體一結構交互作用問題。在無限領域之三維流體運動被以有限領域之二維非穩態流體運動近似之，此時一個更鬆弛的Sommerfeld's Radiaiton Condition被加在有限領域的開境界上。以本文方法所求得之船舶運動流體力係數經與實驗及其他作者之研究結果比較，證實此方法爲一很好且具有發展性之方法。

1. INTRODUCTION

Oceangoing ships are designed to operate in a wave environment. The ship motion problem is not only three-dimensional but also has speed effects.

Since the well-known paper of St. Denis and Pierson [7], with the assumption of small, unsteady motions of the ship and of the surrounding fluid, the ship motion problem can be decomposed linearly into two problems: the radiation problem and the diffraction problem. We can consider separately the radiation problem, where the ship undergoes prescribed oscillatory motions in otherwise calm water, and the diffraction problem, where incident waves act upon the ship in its steady-state equilibrium position.

Strip theory is probably the most widely used method to compute the hydrodynamic forces acting on a vessel in regular waves. The strip theory for heave and pitch motions in head waves of Korvin- Kroukovsky and Jacobs [4] was the first motion theory utilizing the two-dimensional results as an approximation for the three-dimensional ship-motion problem. They solved two-dimensional boundary-value problems for each cross-section of the ship. The two-dimensional solutions were then adjusted to include certain three-dimensional forward speed effects based on intuitive, physical arguments. In general, they satisfactorily agreed with the experimental results, for the heave and pitch motions of the ship in head waves. But the cross-coupling coefficients in the theory did not satisfy the symmetry relations proved by Timman and Newman [8], and that has raised a major objection to this theory. This original strip theory has since been modified and extended by many authors. Salvesen et al. [6] provided another formulation for strip theory with the forward-speed effects through the hull boundary condition. But the free surface condition were independent of the ship's forward speed. The conventional strip theory

does not necessarily give accurate answers (for example, high forward speed or nonconventional vessels), since the forward-speed effects are taken into account only through the hull boundary condition, while the free-surface condition is customarily taken as a time harmonic with no forward-speed dependence. It is a high frequency theory in that the frequency of encounter is assumed large.

Newmann and Tuck (1964) developed the ordinary slender-body theory of ship motions by assuming the frequency to be low. In the theory, the wave length of the incident waves was the same order of magnitude as the ship's length.

Newmann [5] and Sclavounos [14] proposed a so-called unified theory to link ordinary slender body theory and strip theory. At low frequencies, the unified theory approaches the ordinary slender-body theory and yields terms that involve longitudinal interference between sections. For high frequencies, the longitudinal interference disappear and the results are identical to the strip theory. In that theory, the flow fields were divided into two regions; an inner region close to the hull and an outer region far apart from the hull. The flow in the near field was two-dimensional, satisfying the two-dimensional Laplace equation and the linearized time-harmonic free surface condition, together with the hull boundary condition. The fully three-dimensional flow in the outer region satisfied the three-dimensional Laplace equation, subject to the complete linearized free-surface condition and the radiation condition at infinity. The complete solution was obtained by matching outer and inner solutions in a suitably defined overlap region. The unified theory was applied to the forced heave and pitch motions of the ship in head seas. The computational results quite satisfactorily agreed with experimental results. However, it is worthwhile to point out that the free-surface condition in the inner problem did not include

any forward-speed effects, while the hull boundary condition did.

Chapman [20][3] initiated a new approach to solve the three dimensional ship motion problems, which included the forward-speed effects on the free-surface condition. The flow at each cross-section of the ship was analyzed in a quasi-two-dimensional manner along the characteristic lines defined in his formulation, with interaction propagated downstream by the free-surface condition.

Yamasaki & Fujino used Chapman's concept [20] to solve the stability derivatives of a Wigley model [9] and the swaying, yawing and rolling problems of real ship [10].

The advent of large, high-speed computers has allowed the direct numerical solution of some three dimensional seakeeping problems. Chang [2] developed a numerical technique in the frequency domain for calculating the linearized three-dimenisonal ship motion problem. In Chang's fully three-dimensional theory, the effects of forward speed on the free-surface condition were taken into account by modifying the fundamental singularity. Besides, A three-dimensional time-domain seakeeping computer code has been developed by Magee & Beck [15] at the University of Michigan. The code uses linear system theory to determine the hydrodynamic forces acting on a vessel due to forced oscillations (radiation forces) or due to incident waves (exciting forces). It is based on the Neumann-Kelvin potential flow model and solves the problem directly in the time domain rather than the traditional frequency domain. In the Neumann-Kelvin approach the body boundary condition is satisfied on the exact body surface and the linearized free surface condition is used. This approach considers the three-dimensionality of the body surface, but only some of the forward speed effects. The speed effects on the ship surface boundary

condition due to the steady forward motion are made the same approximation used on strip theory. Another three-dimensional time domain approach is developed by Lin & Dick [16] to study the small-amplitude motions and loads of a ship in a seaway, where the linear body and free surface boundary conditions are used , and the large-amplitude motions, where the exact body boundary conditions is satisfied on the instantaneous wetted surface of the moving body while the free-surface boundary conditions are linearized. For problems with forward speed the time-domain solution appear to require less computational effort than the equivalent frequency-domain solution.

The authors [18] have applied Chapman's concept [20] to solve oblique towing flat plate problems before. In this paper, the Chapman's concept [20] is expanded to solve the small heaving and pitching motion problems of a Wigley and a Series 60 ship model moving with speed again.

The present method is an important step forward in the development of ship motions with forward speed under small amplitude. It also supplies the major basis of futual development including nonlinearities in both the body and the free surface boundary condition.

2. PROBLEM FORMULATION

In this problem, the ship model is assumed to be slender. It is executing the heaving and pitching motions with forward speed and the amplitudes of motion are infinitesimal. The model and the coordinate system are shown in Fig.1.

$O_2 - x_2y_2z_2$ is a body-fixed coordinate system with its origin at the intersection of the ship's bow and waterline. Another system $O_1 - x_1y_1z_1$ advances in a straight manner in the mean course of the ship at a forward speed of U. The origin O_1 is located at the intersection of the leading edge of the ship and the undisturbed waterline. The x_1 coordinate is positive in the negative direction of advancing direction of the ship and the z_1 coordinate is positive upward.

The fluid is assumed to be inviscid, incompressible, and irrotational. The flow may be described by a velocity potential

$$\Phi(x_1, y_1, z_1, t) = Ux_1 + \varphi_1(x_1, y_1, z_1, t) \tag{1}$$

In a fluid where U is the advancing speed of the ship, t is time and $\varphi_1(x_1, y_1, z_1, t)$ is the 3-D velocity potential due to the unsteady ship motion, it must satisfy the 3-D Laplace equation.

The three-dimensional Laplace's equation, the kinematic and dynamic conditions of the free-surface, which the velocity potential φ_1 satisfies, are as follows:

$$[L] \quad \frac{\partial^2\varphi_1}{\partial x_1^2} + \frac{\partial^2\varphi_1}{\partial y_1^2} + \frac{\partial^2\varphi_1}{\partial z_1^2} = 0 \quad in \quad fluid \tag{2}$$

$$[K] \quad \frac{\partial\zeta}{\partial t} + (U + \frac{\partial\varphi_1}{\partial x_1})\frac{\partial\zeta}{\partial x_1} + \frac{\partial\varphi_1}{\partial y_1}\frac{\partial\zeta}{\partial y_1} = \frac{\partial\varphi_1}{\partial z_1} \quad on \quad z_1 = \zeta \tag{3}$$

$$[D] \quad \frac{\partial\varphi_1}{\partial t} + U\frac{\partial\varphi_1}{\partial x_1} + \frac{1}{2}\{(\frac{\partial\varphi_1}{\partial x_1})^2 + (\frac{\partial\varphi_1}{\partial y_1})^2 + (\frac{\partial\varphi_1}{\partial z_1})^2\} + g\zeta = 0 \ on \ z_1 = \zeta \tag{4}$$

where ζ is the elevation of the free surface and g the acceleration of gravity.

Chapman [20][3] assumed that if a 3-D body is slender, the 3-D fluid motion around the slender body can be approximated by the unsteady 2-D flow in a space-fixed plane normal to the longituinal axis of the body. The 3-D velocity potential $\varphi_1(x_1, y_1, z_1, t)$ can be approximated by the unsteady 2-D velocity potential $\varphi(y_1, z_1, t)$ in the $y_1 z_1$ plane, and $\varphi(y_1, z_1, t)$ satisfies the 2-D Laplace equation. In fluid

$$[L] \quad \frac{\partial^2 \varphi}{\partial y_1^2} + \frac{\partial^2 \varphi}{\partial z_1^2} = 0 \tag{5}$$

Since the motions of the ship are assumed to be infinitesimal, the higher order terms in Eqs. (3) and (4) can be neglected and the problem can be linearized. The linearized free surface kinematic boundary condition in the $y_1 z_1$ plane becomes

$$[K] \quad (\frac{\partial}{\partial t} + U\frac{\partial}{\partial x_1})\zeta = \frac{\partial \varphi}{\partial z_1} \quad on \quad z_1 = 0 \tag{6}$$

The linearized free surface dynamic boundary condition in the $y_1 z_1$ plane is

$$[D] \quad (\frac{\partial}{\partial t} + U\frac{\partial}{\partial x_1})\varphi + g\zeta = 0 \quad on \quad z_1 = 0 \tag{7}$$

For the linear problem, it is assumed that the potential is symmetric about $y_1 = 0$. Then, the condition under the ship in the $y_1 z_1$ plane becomes

$$\frac{\partial \varphi}{\partial y_1} = 0 \tag{8}$$

Based on the assumption that heaving motions h(t) and pitching motions a(t) of the model are infinitesimal, the coordinate systems, $O_1 - x_1 y_1 z_1$ and $O_2 - x_2 y_2 z_2$, have the following relations:

$$x_2 = x_1 - z_1 a(t) \tag{9}$$

$$y_2 = y_1 \tag{10}$$

$$z_2 = z_1 - h(t) - (x_G - x_1)a(t) \tag{11}$$

where x_G is the horizontal distance from the ship's bow to the center of gravity. $h(t)$ is the pure heaving motion. $a(t)$ is the pure combination motion.

Let the hull shape be represented by

$$H(x_2, y_2, z_2) = 0 \tag{12}$$

then the body surface condition is described by

$$\dot{x}_2 \frac{\partial H}{\partial x_2} + \dot{y}_2 \frac{\partial H}{\partial y_2} + \dot{z}_2 \frac{\partial H}{\partial z_2} = 0 \quad on \quad H(x_2, y_2, z_2) = 0 \tag{13}$$

Considering that the ship's motion is small, the body surface condition can be satisfied on mean ship hull surface $H(x_1, y_1, z_1) = 0$ rather than on the exact ship hull surface. By substituting Eqs.(1), (9), (10) and (11) into (13), the body surface condition at the mean hull surface may be expressed as follows:

$$[H] \quad U\frac{\partial H}{\partial x_1} + \frac{\partial \varphi}{\partial y_1}\frac{\partial H}{\partial y_1} + \frac{\partial \varphi}{\partial z_1}\frac{\partial H}{\partial z_1} = [\dot{h}(t) - Ua(t) + (x_G - x_1)\dot{a}(t)]\frac{\partial H}{\partial z_1}$$

$$on \quad H(x_1, y_1, z_1) = 0 \tag{14}$$

The two characteristic lines in the $x_1 - t$ plane are defined by

$$t - x_1/U = constant \tag{15}$$

$$t + x_1/U = constant \tag{16}$$

The position of a point on a characteristic line is specified by

$$\bar{s} = \frac{1}{2}(t + x_1/U) \tag{17}$$

$$\bar{q} = \frac{1}{2}(t - x_1/U) \tag{18}$$

According to Eqs.(17) and (18)

$$t = \bar{s} + \bar{q} \tag{19}$$

$$x_1 = U(\bar{s} - \bar{q}) \tag{20}$$

According to the chain rule, then

$$(\frac{\partial}{\partial t} + U\frac{\partial}{\partial x_1}) = \frac{\partial}{\partial \bar{s}} \tag{21}$$

Substituting Eq. (21) into Eqs. (6), (7) and (14) , Eqs. (5), (6), (7) and (14) along the characteristic lines may be expressed as follows

$$[L] \quad \frac{\partial^2\varphi}{\partial y_1^2} + \frac{\partial^2\varphi}{\partial z_1^2} = 0 \quad in\ fluid \tag{22}$$

$$[K] \quad \frac{\partial\zeta}{\partial\bar{s}} = \frac{\partial\varphi}{\partial z_1} \quad on \quad z_1 = 0 \tag{23}$$

$$[D] \quad \frac{\partial\varphi}{\partial\bar{s}} + g\zeta = 0 \quad on \quad z_1 = 0 \tag{24}$$

$$[H] \quad \frac{\partial \varphi}{\partial y_1}\frac{\partial H}{\partial y_1} + \frac{\partial \varphi}{\partial z_1}\frac{\partial H}{\partial z_1} = -U\frac{\partial H}{\partial x_1} + [\dot{h}(\bar{s}+\bar{q}) - Ua(\bar{s}+\bar{q}) + (x_G - x_1)$$
$$\dot{a}(\bar{s}+\bar{q})]\frac{\partial H}{\partial z_1} \qquad on \quad H(x_1, y_1, z_1) = 0 \tag{25}$$

The open boundary condition is [10]

$$[O] \quad \frac{\partial \varphi}{\partial \bar{s}} + C\frac{\partial \varphi}{\partial l} = E \quad on\ the\ open\ boundary. \tag{26}$$

where C is the propagation speed of the wave, l is the direction normal to the open boundary, and E is the numerical error for Sommerfeld radiation condition.

3. HEAVING FORCES AND PITCHING MOMENTS

Through the boundary element method calculation, the velocity potential φ on the boundaries along the characteristic lines can be obtained.

The hydrodynamic vertical force f(T, X) acting on a ship's section, which is situated in the 2-D transverse plane along the characteristic lines at $x_1 = X$, at the instant t = T, are expressed by

$$f(T,X) = -2\rho \int_K^F \frac{\partial \varphi}{\partial \bar{s}} n_z ds \tag{27}$$

where ρ is fluid density, $n = (n_y, n_z)$ is a normal inward unit vector of the ship's hull. K is the keel location. F is the undisturbed water line. ds is a line segment along the hull surface.

Contour integration is performed along the surface of the hull from the keel to the intersection of the hull and undisturbed waterline.

Consequently, the hydrodynamic vertical force Y(T) acting on the entire ship at the same instant t = T are obtained by integrating Eq.(27) over the ship's length.

$$Y(T) = \int_o^L f(T,x)dx \tag{28}$$

The hydrodynamic moment N(T) acting on the entire ship at the instant t = T are obtained by Eq.(27) over the ship's length.

$$N(T) = \int_o^L f(T,x)x dx \tag{29}$$

where L is the length of Wigley or series 60 ship model.

Then the hydrodynamic vertical force time series Y(t) and the hydrodynamic moment time series N(t) can be obtained.

4. DETERMINATION OF HYDRODYNAMIC COEFFICIENTS

§ Forced Pure Heaving Motions:

When the forced pure heaving motions are considered, the equations of motion are :

$$A_{33}\ddot{h}(t) + B_{33}\dot{h}(t) = Y(t) \tag{30}$$

$$A_{53}\ddot{h}(t) + B_{53}\dot{h}(t) = N(t) \tag{31}$$

where $h(t) = z_a \sin\omega t$

z_a : The amplitude of pure heaving motion.

ω: The frequency of pure heaving motion.

A_{33}: Heave diagonal added mass.

B_{33}: Heave diagonal damping coefficients.

A_{53}: Heave and pitch off-diagonal added mass.

B_{53}: Heave and pitch off-diagonal damping coefficients.

Through the Fourier Series expansion, the hydrodynamic coefficients A_{33}, B_{33}, A_{53} and B_{53} can be calculated. The nondimensional hydrodynamic coefficients are calculated as follows

$$A'_{33} = A_{33}/\rho\nabla \tag{32}$$

$$B'_{33} = B_{33}\sqrt{L/g}/\rho\nabla \tag{33}$$

$$A'_{53} = A_{53}/\rho\nabla L \tag{34}$$

$$B'_{53} = B_{53}\sqrt{L/g}/\rho\nabla L \tag{35}$$

where ∇ is the displacement volume of Wigley or series 60 ship model.

§ Forced Combination Motions:

When the forced combination motions are considered, the equations of motion are :

$$A_{35}\ddot{a}(t) + B_{35}\dot{a}(t) = Y(t) \tag{36}$$

$$A_{55}\ddot{a}(t) + B_{55}\dot{a}(t) = N(t) \tag{37}$$

where $a(t) = \theta_a \sin \omega t$

θ_a : The amplitude of combination motion.

ω : The frequency of combination motion.

A_{35}: Heave and pitch off-diagonal added mass.

B_{35}: Heave and pitch off-diagonal damping coefficients.

A_{55}: Pitch diagonal added mass.

B_{55}: Pitch diagonal damping coefficient.

Through the Fourier Series expansion, the hydrodynamic coefficients A_{35}, B_{35}, A_{55} and B_{55} can be calculated. The nondimensional hydrodynamic coefficients are obtained as follows

$$A'_{35} = A_{35}/\rho\nabla L \tag{38}$$

$$B'_{35} = B_{35}\sqrt{L/g}/\rho\nabla L \tag{39}$$

$$A'_{55} = A_{55}/\rho\nabla L^2 \tag{40}$$

$$B'_{55} = B_{55}\sqrt{L/g}/\rho\nabla L^2 \tag{41}$$

5. NUMERICAL METHOD

§ Formulation of Boundary Element Equation:

For a given 'i' point of constant element, the next boundary equation exists [19]

$$\frac{1}{2}u^i + \sum_{j=1}^{N} u_j \int_{\Gamma_j} q^* d\Gamma = \sum_{j=1}^{N} q_j \int_{\Gamma_j} u^* d\Gamma \tag{42}$$

where $u^* = (1/2\pi)\ ln\ (1/r)$ is the fundamental solution of isotropic two dimensional Laplace equation. r is the distance from the point of application of the delta function to the point under consideration. u^i is the value of u^* during r = 0. u_j is the value of velocity potential on the segment 'j'. q_j is the value of velocity potential derivative on the segment 'j'. Γ is the close boundary of the computational domain. n is the unit normal vector of the boundary. $q = \partial u/\partial n$, $q^* = \partial u^*/\partial n$. The terms $\int_{\Gamma_j} q^* d\Gamma$ and $\int_{\Gamma_j} u^* d\Gamma$ relate the 'i' node with the segment 'j' over which the integral is carried out.

The values of u and q are assumed to be constant on each constant element and equal to the value at the mid-node of the element. The above integrals are easy to calculate, the velocity potential and it's derivative along the boundary can be obtained.

§ Discretization of Free Surface Boundary Condition:

The discretized forms of the free surface kinematic and dynamic boundary conditions on characteristic line $\bar{s}$ are modified from [10]:

$$\zeta(y_1 + \frac{\triangle y_1}{2}, \bar{s} + \frac{\triangle \bar{s}}{2}, \bar{q}) = \zeta(y_1 - \frac{\triangle y_1}{2}, \bar{s} - \frac{\triangle \bar{s}}{2}, \bar{q}) + \triangle \bar{s} \frac{\partial \varphi}{\partial z_1}(y_1, 0, \bar{s}, \bar{q}) \tag{43}$$

$$\varphi(y_1+\triangle y_1,0,\bar{s}+\triangle\bar{s},\bar{q})=\varphi(y_1,0,\bar{s},\bar{q})-g\triangle\bar{s}\zeta(y_1+\frac{\triangle y_1}{2},\bar{s}+\frac{\triangle\bar{s}}{2},\bar{q}) \qquad (44)$$

where $\triangle\bar{s}$ is the length spacing along the characteristic line $\bar{s}$ and

$$\triangle y_1=\triangle\bar{s}\frac{\partial\varphi}{\partial y_1}(y_1,0,\bar{s},\bar{q}) \qquad (45)$$

§ Discretization of Open Boundary Condition:

The open boundary condition, Eq. (26), is treated by an upwind-centered difference scheme [1]. For point I, as shown in Fig.2, the difference form of Sommerfeld's radiation condition on characteristic line $\bar{s}$ are modified from [10]:

$$[P(\tau+1.1)-P(\tau,1)+P(\tau,2)-P(\tau-1,2)]/2+\alpha[P(\tau,1)-P(\tau,2)]=\epsilon \quad (46)$$

where $\alpha=C\triangle\bar{s}/\triangle l, \epsilon=E\triangle\bar{s}$, τ denotes the position on the characteristic line, $\triangle l$ is the grid spacing in the direction normal to the open boundary, and $P(\tau,J)$ is the velocity potential. For point II, the difference form of Sommerfeld's radiation condition is

$$[P(\tau,2)-P(\tau-1,2)+P(\tau-1,3)-P(\tau-2,3)]/2+\alpha^*[P(\tau-1,2)-P(\tau-1,3)]=\epsilon^* \qquad (47)$$

For point III, the difference form of Sommerfeld's radiation condition is

$$[P(\tau-1,3)-P(\tau-2,3)+P(\tau-2,4)-P(\tau-3,4)]/2+\alpha^*[P(\tau-2,3)-P(\tau-2,4)]=\epsilon^* \qquad (48)$$

Since in Eqs.(47) and (48) P is known, α^* and ϵ^* can be computed

$$\alpha=0 \qquad as \quad \alpha^*<0$$

$$\alpha=\alpha^*,\epsilon=\epsilon^* \quad as \quad 0\le\alpha^*\le 1$$

$$\alpha = 1 \qquad as \quad \alpha^* > 1$$

For the case of $\alpha^* < 0$ or $\alpha^* > 1$, α^* is set to 0 or 1 in Eqs. (47) and (48), then two ϵ^*, i.e. $\epsilon_1^*, \epsilon_2^*$ are determined, and $\epsilon = (\epsilon_1^* + \epsilon_2^*)/2$. With α and ϵ determined $P(\tau + 1.1)$ can be computed from Eq.(46).

6. DETERMINATION OF MESH SIZE

According to Eqs. (17) and (18), along the characteristic line $\bar{s}$, $\bar{q}$ is a constant. The time step $\triangle t$ is taken to be $\triangle x_1/U$. Then $\triangle \bar{s}$ equals to $\triangle t$.

For the free surface boundary condition,

$$\frac{\partial^2 \varphi}{\partial \bar{s}^2} + g\frac{\partial \varphi}{\partial z_1} = 0 \quad on\ z_1 = 0.$$

As $\triangle \bar{s} \leq \beta\sqrt{\triangle z_1/g}$, $\beta = 1$, the numerical solution will converge. Here, we take the time steps equal to 81 in the characteristic line $\bar{s}$ direction and the line segment in the z_1 direction equal to 40, the above criteria can be satisfied.

7. NUMERICAL PROCEDURE

Fig. 3 shows the fluid domain used in the numerical simulation. The simulation procedure is summaried as follows.

1. At $\bar{s} = 0$, the fluid is assumed to be at rest, and φ on the free surface and the open boundary equals to zero. At the boundary under the keel, $\partial\varphi/\partial y_1 = 0$.
2. The 2-D flow field is solved by boundary element method to satisfy the body surface boundary condition. Then, the φ on body surface and $\partial\varphi/\partial z_1$ on free surface can be calculated.
3. The value of φ at the internal points adjacent to the open boundary is calculated. The value of φ on the open boundary at the next step $\bar{s} = \bar{s} + \triangle\bar{s}$ is then obtained.
4. The velocity potential φ on the free surface at the step $\bar{s} = \bar{s} + \triangle\bar{s}$ is determined by the free surface boundary condition.
5. The free surface are again subjected to division because the hull shape at $\bar{s} = \bar{s} + \triangle\bar{s}$, is different from that at $\bar{s} = \bar{s}$.
6. The velocity potential φ at the new nodal points on free surface is determined by linear interpolation of φ values obtained at the step 4.
7. Return to the step 2 recursively.

The spline interpolation method is used to estimate the sectional shapes of the Wigley or ship model's hull, which are not given in the body plan. To carry out the numerical simulation in an efficient manner, the propeller aperture behind the stern frame was filled with a hypothetical piece of dead wood as illustrated in Fig. 12 [10].

8. NUMERICAL RESULTS AND DISCUSSION

The pure heaving and forced combination motions of Wigley and Series 60 ship model are carried out by numerical simulation. The main particulars are given in Tables 1 and 2 respectively.

The computational domain is taken to be 8 times of draft. The amplitude of pure heaving and combination motion are 0.025 M, and 0.026 radian respectively. The Froude number in length Fn ($= U/\sqrt{gL}$) =0.2. The total boundary element number is 200. The time steps are 81.

Fig. 4 $\sim$ Fig. 11 and Fig. 13 $\sim$ Fig. 20 show the heave and pitch diagonal and off-diagonal added mass and damping coefficients of Wigley model and Series 60 ship model individually.

a. Wigley model

The half beam y_1 of Wigley model is given by:

$$\frac{y_1}{b} = (1-X)(1-Z)(1+0.2X) + Z(1-Z^4)(1-X)^4$$

where $X = (2x_1 - L)^2/L^2$, $Z = (z_1/H)^2$, $b = B/2$.

The frequencies (rad/sec) of Wigley model motion used to do numerical simulation are 2.271, 2.455, 3.133, 3.63, 4.126, 5.047, 6.489, 7.5706 and 9.085 individually.

The nondimensional heave diagonal added mass A'_{33} of the experiment value in Fig. 4 quickly decrease from the frequency 3.133 rad/sec, then gradually become a stable value at the higher frequency, that is to say, they almost approach constant at the frequency higher than 5.047 rad/sec. The present and all other methods have good coincidence with the experiment results at higher frequency , but the present method has better trend to the experiment than all other methods at the lower frequency.

The nondimensional heave diagonal damping coefficients B'_{33} of the experiment value in Fig. 5 have larger value near the frequency 3.63 rad/sec. The present and all other methods almost have the same trend with the experiment results, but the coincidence only occur at the higher frequency.

The nondimensional heave and pitch off-diagonal added mass A'_{53} of the experiment value in Fig. 6 quickly decrease at the frequency near 2.271 rad/sec towards the higher frequency. All the methods have similar trend with the experiment results. The present method shows closer results to the experiment than Strip theory and small amplitude calculations of Lin & Dick [16].

The nondimensional heave and pitch off-diagonal damping coefficients B'_{53} in Fig. 7 show that all the methods have similar trend with the experiment

results, but the present method can give better results to the experiment results than small amplitude calculations of Lin & Dick.

The nondimensional heave and pitch off-diagonal added mass A'_{35} are shown in Fig. 8. As the frequency is larger than 6.489 rad/sec, the experiment value of A'_{35} approaches a constant value, and the results of present method, Magee & Beck [15] and small amplitude calculations of Lin & Dick can give almost the same value. All the methods have similar trend with the experiment results.

The nondimensional heave and pitch off-diagonal damping coefficients B'_{35} are shown in Fig. 9. As the frequency is larger than 6.489 rad/sec, the results of present method, Magee & Beck [15] and Strip theory [6] can all give almost the same value as experiment. All the methods have similar trend with the experiment results, but, the results of small amplitude calculations of Lin & Dick [16] predict smaller value than all other method.

The nondimensional pitch diagonal added mass A'_{55} are shown in Fig. 10. As the frequency is larger than 5.047 rad/sec, the experiment value of A'_{55} approaches a constant value. In this frequency range, all the methods can give similar value, but, the results of the present method are better than all other methods. All the methods have similar trend with the experiment results.

The nondimensional pitch diagonal damping coefficients B'_{55} are shown in Fig. 11. As the frequency is larger than 7.5706 rad/sec, the value of B'_{55} of the experiment, present and all other methods approach a close value. Besides, except the Strip theory [6], all the other methods have similar trend with the experiment results.

On the whole, for A'_{33}, A'_{53}, A'_{35}, A'_{55} and B'_{55}, the result calculated by the present method are closer to the experiment than those done by the Strip

theory, especially, the B'_{55} of the latter is bad. For B'_{33}, B'_{53} and B'_{35}, the result calculated by the present method and Strip theory are close to the experiment in the same order.

For A'_{33} and A'_{55}, the present method can predict closer value to experiment than Magee & Beck's. For B'_{33}, A'_{53}, B'_{53}, A'_{35}, B'_{35} and B'_{55}, the result calculated by the present and Magee & Beck's method are close to the experiment in the same order.

For A'_{33}, A'_{53}, B'_{53} and B'_{35}, the present method is better than small amplitude calculations of Lin & Dick, especially, the B'_{35}. For B'_{33}, A'_{35}, A'_{55} and B'_{55}, the present and Lin & Dick's method are almost closer to the experiment in the same order.

From the above analysis, we know the present method is a very good method for the calculation of the heave and pitch diagonal and off-diagonal added mass and damping coefficients of the Wigley model.

b. Series 60 ship model

The frequencies (rad/sec) of Series 60 model motion are 2.618, 2.830, 3.611, 4.189, 4.760, 5.818, 7.480, 8.727 and 10.472 respectively.

The nondimensional heave diagonal added mass A'_{33} of the experiment value in Fig. 13 become a little stable from the frequency 5.818 rad/sec towards the higher frequency, that is to say, they almost approach constant at the higher frequency. The present and all other methods have good coincidence with the experiment results.

The nondimensional heave diagonal damping coefficients B'_{33} of the experiment value in Fig. 14 have larger value near the frequency 4.760 rad/sec and quickly decrease as the frequency is higher. The present and all other methods almost have the same trend with the experiment results.

At the frequency near 2.618 rad/sec, the calculated nondimensional heave and pitch off-diagonal added mass A'_{53} in Fig. 15 quickly decrease towards higher frequency, but the experiment values only decrease slowly. All the methods have similar trend with the experiment results, and the coincidence still only occur at the higher frequency. The present method shows better results than all other method.

The nondimensional heave and pitch off-diagonal damping coefficients B'_{53} in Fig. 16 show that all the methods have similar trend with the experiment results, but the present method can give closer results to the experiment results than Strip theory and Unified theory [14]. The present method and Magee & Beck's calculation [15] are almost closer to the experiment in the same order.

The nondimensional heave and pitch off-diagonal added mass A'_{35} are shown in Fig. 17. As the frequency is larger than 7.480 rad/sec, the experiment value of A'_{35} approaches a constant value, the present method can give almost

the same value. The results of Strip and Unified theory can obtain the close value, but a little lower. Magee & Beck can obtain the close value, but a little higher. The present and all other methods have similar trend with the experiment results.

The nondimensional heave and pitch off-diagonal damping coefficients B'_{35} are shown in Fig. 18. As the frequency is larger than 8.727 rad/sec, the experiment value of B'_{35} approaches a constant value. The present and all other methods have similar trend with the experiment results. Near the frequency 2.830 rad/sec, the present method can predict close value to the experiment value, but, it predict larger value than the experiment at higher frequency.

The nondimensional pitch diagonal added mass A'_{55} are shown in Fig. 19. As the frequency is larger than 5.818 rad/sec, the experiment value of A'_{55} approaches a constant value. The present method can predict close value to the experiment as the frequency is higher than 7.480 rad/sec. All the methods have similar trend with the experiment results.

The nondimensional pitch diagonal damping coefficients B'_{55} are shown in Fig. 20. The present method can predict closer value to the experiment than all other methods.

On the whole, for A'_{53}, B'_{53}, A'_{35} and B'_{55} of Series 60 model calculated by the present method are closer to the experiment than those done by the Strip theory, especially, the B'_{55}. For B'_{33} and B'_{35}, the results calculated by the present method and Strip theory are close to the experiment in the same order. For A'_{33} and A'_{55}, the Strip theory can predict closer value to experiment than the present method.

For B'_{33}, A'_{53} and B'_{55}, the present method can predict closer value to experiment than Magee & Beck's, especially, the B'_{55}. For A'_{33}, B'_{53}, A'_{35} and

A'_{55}, the result calculated by the present and Magee & Beck's method are close to the experiment in the same order.

For B'_{33}, A'_{53}, B'_{53}, A'_{35} and B'_{55}, the present method can predict closer value to experiment than Unified theory [14]. For A'_{33}, B'_{35} and A'_{55}, the Unified theory can predict closer value to experiment than the present method.

Therefore the present method is a good method for the calculation of the heave and pitch diagonal and off-diagonal added mass and damping coefficients of Series 60 ship model.

Table 1

Main Particulars of the Wigley model

Length between perpendiculars L	3.000 m
Breadth B	0.300 m
Draught d	0.1875 m
Trim	0.000 m
Volume of displacement ∇	0.0946 m^3
Coefficient of mid-length section C_M	0.909
Center of rotation above base	0.1875 m
Center of gravity above base	0.170 m
Radius of inertia for pitch	0.750 m
Froude number of service speed	0.20

Table 2

Main Particulars of the Series 60 ship model

Length between perpendiculars L	2.258 m
Length on the waterline	2.296 m
Breadth B	0.322 m
Draught d	0.129 m
Volume of displacement ∇	0.0657 m^3
Block coefficient C_B	0.700
Coefficient of mid-length section C_M	0.986
Prismatic Coefficient C_P	0.710
Waterplane area	0.572 m^2
Waterplane Coefficient C_W	0.785
Longitudinal moment of inertia of waterplane	0.1685 m^4
L.C.B. forward of $L_{BP}/2$	0.011 m
Center of effort of waterplane after $L_{BP}/2$	0.038 m
Froude number of service speed	0.20

9. CONCLUSIONS

From the above analysis, we know, in general, the heave and pitch diagonal and off-diagonal added mass and damping coefficients of Wigley and Series 60 ship model calculated by the present method are compared well and have the same trend as the experimental and other authors' results.

The present method is a very good method for the calculation of the heave and pitch diagonal and off-diagonal added mass and damping coefficients of Wigley model and Series 60 ship model moving with speed.

It is an important step forward in the development of ship motions with forward speed under small amplitude. It also supplies the major basis of futual development including of nonlinearities in both the body and the free surface boundary condition.

ACKNOWLEDGEMENT

Financial support of this work by National Science Council Grant NSC82-0209-E-124-006 is gratefully acknowledged.

NOMENCLATURE

C	propagation speed of the wave
B	Wigley or ship model breadth
b	Wigley or ship model half breadth
d	Wigley or ship model draft
C_B	Block coefficient
C_M	Coefficient of mid-length section
C_P	Prismatic Coefficient
E	numerical error for the Sommerfeld Radiation Condition
$Y(t)$	resultant vertical force time series
F_n	Froude number in length $(= U/\sqrt{gL})$
g	gravitational acceleration
L	Wigley or ship model length
l	direction normal to the open boundary
$N(t)$	resultant moment time series
P	2-D velocity potential due to the unsteady Wigley or ship model motion
t	time variable
X	x_1 coordinate of calculating 2 D plane
T	the time corresponding to the location $x_1 = X$
U	advancing speed of the Wigley or ship model
x_1, y_1, z_1	x_1, y_1, z_1 coordinates for the coordinate system $O_1 - x_1 y_1 z_1$
z_a	the amplitude of pure heaving motion.
θ_a	The amplitude of combination motion.
ω	The frequency of pure heaving or combination motion

A_{33}	Heave diagonal added mass.
B_{33}	Heave diagonal damping coefficients.
A_{53}	Heave and pitch off-diagonal added mass.
B_{53}	Heave and pitch off-diagonal damping coefficients.
A_{35}	Heave and pitch off-diagonal added mass.
B_{35}	Heave and pitch off-diagonal damping coefficients.
A_{55}	Pitch diagonal added mass.
B_{55}	Pitch diagonal damping coefficient.
A'_{33}	Nondimensional heave diagonal added mass.
B'_{33}	Nondimensional heave diagonal damping coefficients.
A'_{53}	Nondimensional heave and pitch off-diagonal added mass.
B'_{53}	Nondimensional heave and pitch off-diagonal damping coefficients.
A'_{35}	Nondimensional heave and pitch off-diagonal added mass.
B'_{35}	Nondimensional heave and pitch off-diagonal damping coefficients.
A'_{55}	Nondimensional pitch diagonal added mass.
B'_{55}	Nondimensional pitch diagonal damping coefficient.

Greek symbols

ζ	free surface elevation
ρ	mass density of the fluid
∇	volume of displacement
Φ	3-D velocity potential due to the Wigley or ship motion
φ_1	3-D velocity potential due to the unsteady Wigley or ship motion
φ	2-D velocity potential due to the unsteady Wigley or ship

	motion
$\triangle t$	time spacing
$\triangle y$	grid spacing in the y direction
$\triangle z$	grid spacing in the z direction
$\triangle \bar{s}$	the length spacing along the characteristic line $\bar{s}$

References

1. Chan, K. C., "Finite Difference Simulation of the Planar Motion of a Ship", 2nd Int. Conf. on Numer. Ship Hydrodyn., Univ. California, Berkeley (1977).

2. Chang, M. S., "Computations of Three-Dimensional ship Motions with Forward Speed", 2nd Int. Conf. on Numer. Ship Hydrodyn., Univ. California, Berkeley, pp. 124-135 (1977).

3. Chapman, R.B.,"Free Surface Effects for Yawed Surface - Piercing Plates", J. Ship Res., Vol.20, No.30 , (1976).

4. Korvin-Kroukovsky, B.V. and W.R. Jacobs, "Pitching and Heaving Motions of a Ship in Regular Waves", Trans. SNAME, Vol. 65. pp. 590-632 (1957).

5. Newman, J.N., "The Theory of Ship Motions", Adv. Appl. Mech., Vol. 18, pp.221-283 (1978).

6. Salvesen, N., E.O. Tuck and O. Faltinsen, "Ship Motions and Sea Loads", Trans. SNAME, Vol. 78, pp.250-287 (1970).

7. St. Denis, M. and W.J. Pierson, "On the Motion of Ships in Confused Seas", Trans. SNAME, Vol. 61, pp. 280-354 (1953).

8. Timman, R. and J.N. Newman, "The Coupled Damping Coefficients of Symmetric Ships", J. Ship Res., Vol. 5, No. 4, pp. 34-55 (1962).

9. Yamasaki, K., M. Fujino , "Hydrodynamic Forces Acting on the Three Dimensional Body Advancing on the Free Surface (2nd report)", Journal of the Society of Naval Architects of JAPAN, (1984).

10. Yamasaki, K., M. Fujino , "Hydrodynamic Forces Acting on the Three

Dimensional Body Advancing on the Free Surface (3rd report)", Journal of the Society of Naval Architects of JAPAN, (1985).

11. Gerritsma,J., "Ship motions in Longitudinal Waves," International Shipbuilding Progress, No.66, 1960, pp.42-95.

12. Gerritsma,J., and W. Beukelman, "The Distribution of the Hydrodynamic Forces on a Heaving and Pitching Shipmodel in Still Water, "Report No.22, Shipbuilding Laboratory, Technische Hogeschool Delft, Delft, Netherlands, 1964.

13. Gerritsma,J., "Motions, Wave Loads and Added Resistance in Waves of Two Wigley Hull Forms," Delft University of Technology, Shiphydromechanics Laboratory, Report No 804, November 1988.

14. Sclavounos, P.D., "The Unified Slender-Body Theory:Ship Motions in Waves," Proceedings of the Fifteenth Symposium on Naval Hydrodynamics, Hamburg, Germany, 1984, pp.177-193.

15. Magee, A.R. and Beck, R.F., "Compendium of Ship Motion Calculations using Linear Time-Domain Analysis," Report No 310, Department of Naval Architecture and Marine Engineering, College of Engineering, The University of Michigan , Ann Arbor, Michigan 48104, 1988.

16. Lin, W.-M. and D. Yue, "Numerical Solutions for Large-Amplitude Ship Motion in the Time Domain," Proceedings of the 18th Symposium on Naval Hydrodynamics, Ann Arbor, Michigan, 1990.

17. Ir. J.M.J. Journee, "Experiment and Calculations on Four Wigley Hullforms," Report No 909, Ship Hydromechanics Laboratory, Delft University of Technology, Delft, Netherlands, February, 1992.

18. Horng,S.J.,Chiu,F.C. and C.T.,Wang, "Free Surface Effects on an oblique

towing flat plate," Journal of the Chinese Institute of Engineers, Vol. 16, No. 3, pp. 441-450, Taipei, Taiwan, 1993.

19. C.A. Brebbia, "The Boundary Element Method for Engineering," Pentech Press, 1980.

20. Chapman, R. B., "Numerical Solution for Hydrodynamic Forces on a Surface-Piercing Plate Oscillating in Yaw and Sway," 1st Int. Conf. on Numer. Ship Hydrodyn., 1975.

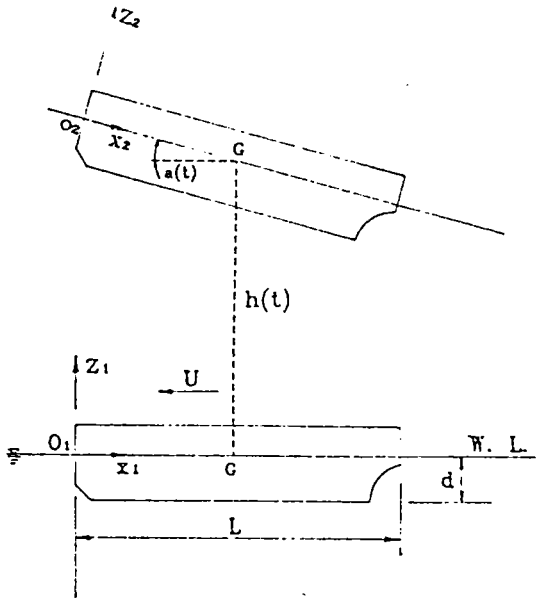

Side View

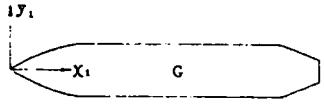

Top View

Fig. 1 Coordinate systems

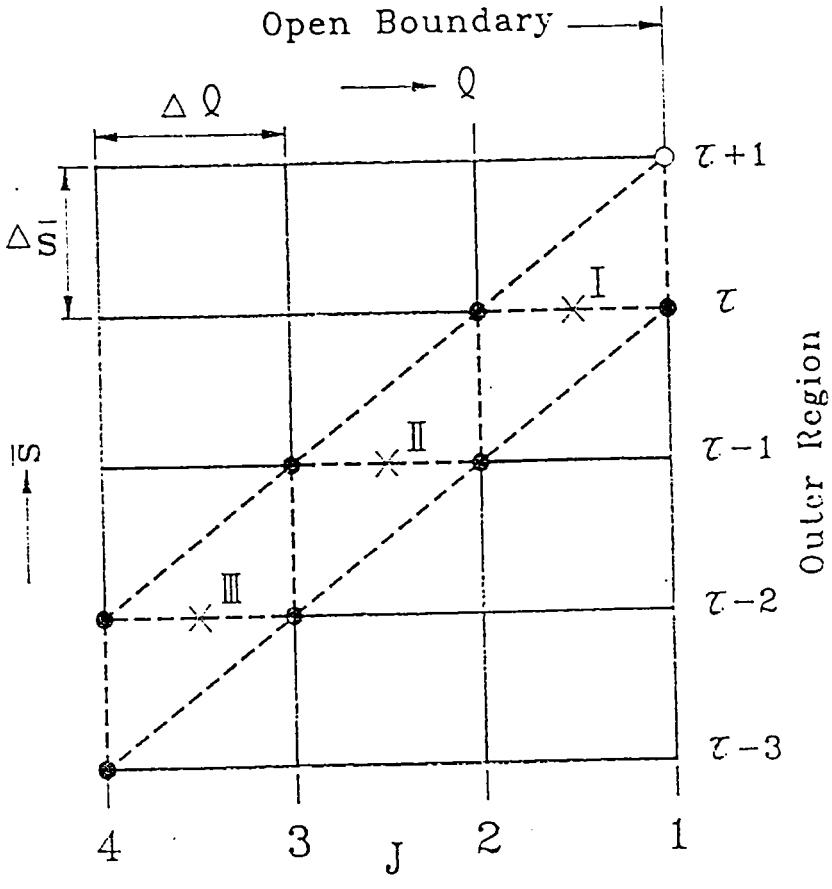

Fig. 2 Discretization on the open boundaries

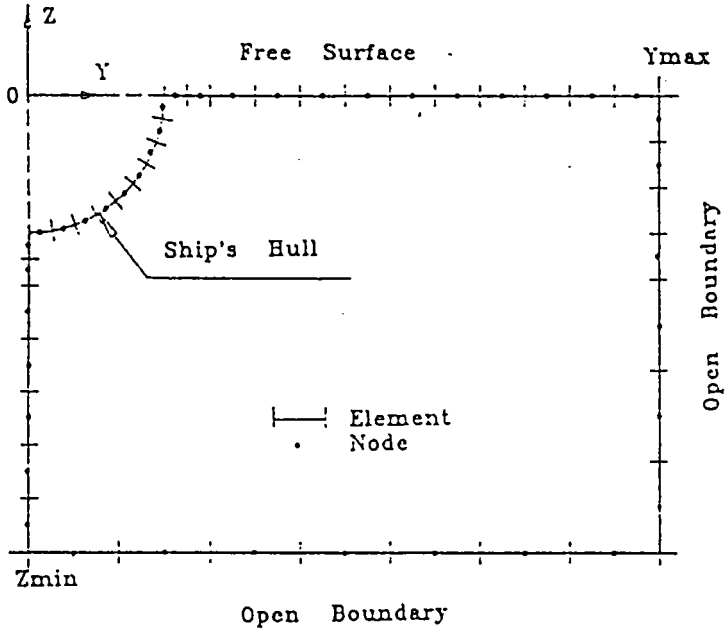

Fig. 3 Boundary elements on the boundaries

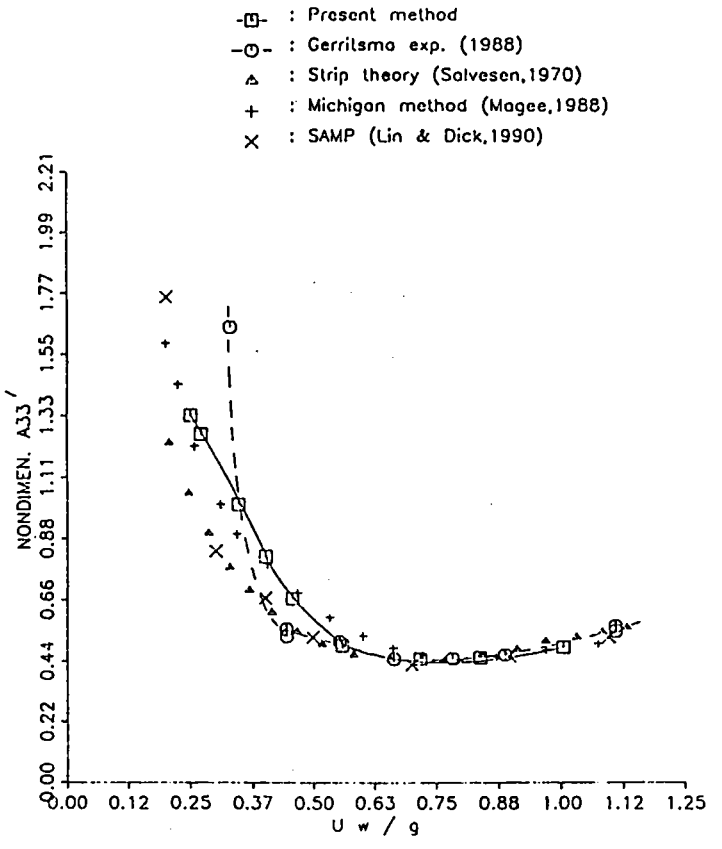

Fig. 4 Nondimensional A'_{33} of Wigley model

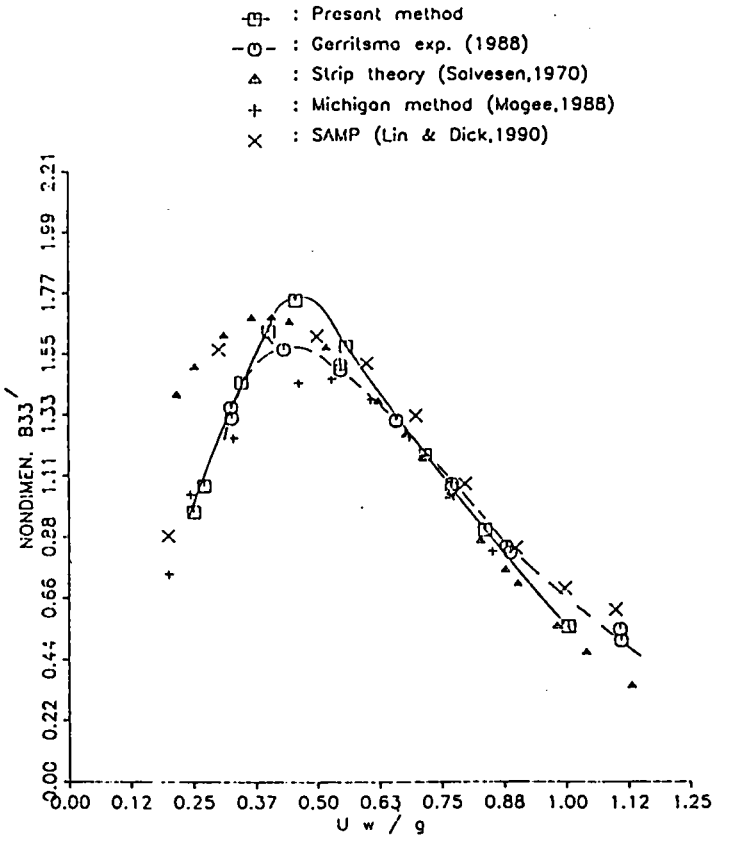

Fig. 5 Nondimensional B'_{33} of Wigley model

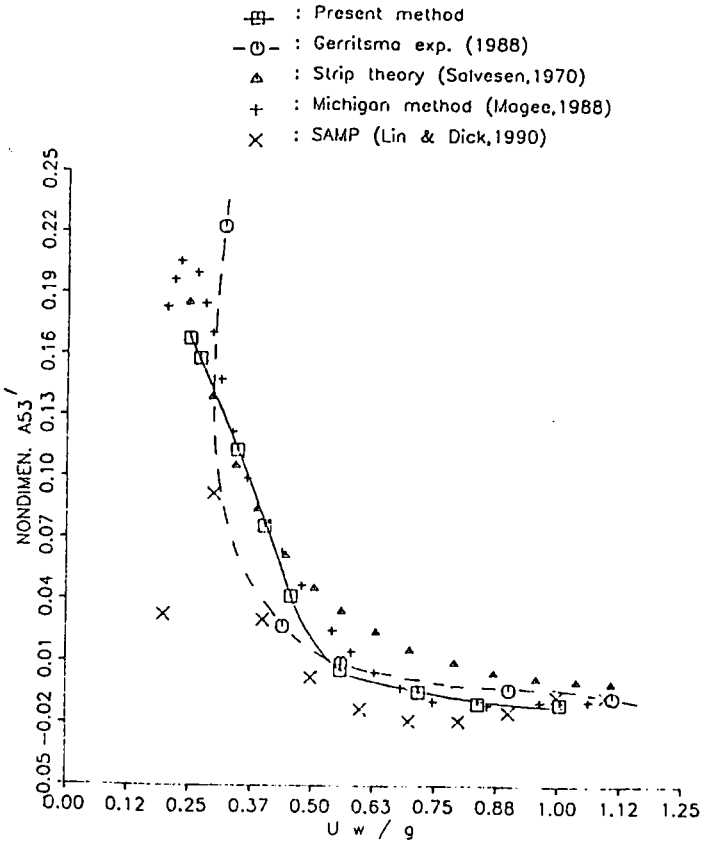

Fig. 6 Nondimensional A'_{53} of Wigley model

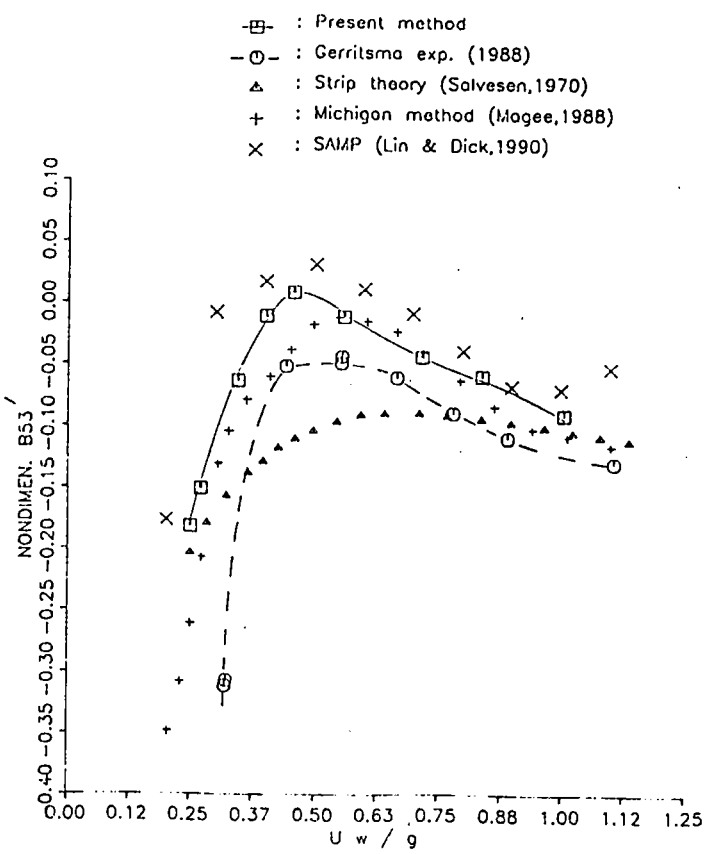

Fig. 7 Nondimensional B'_{53} of Wigley model

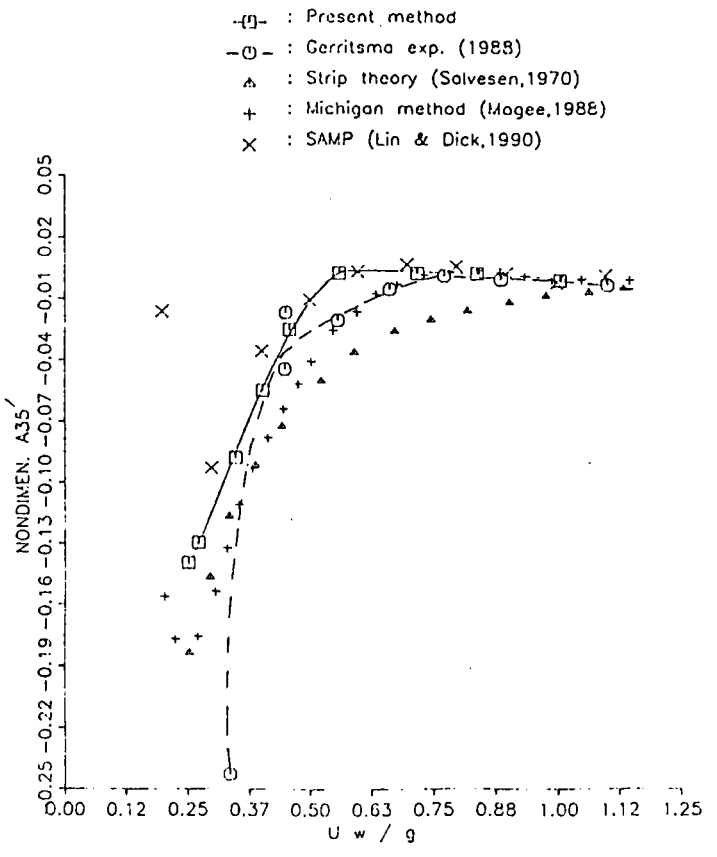

Fig. 8 Nondimensional A'_{35} of Wigley model

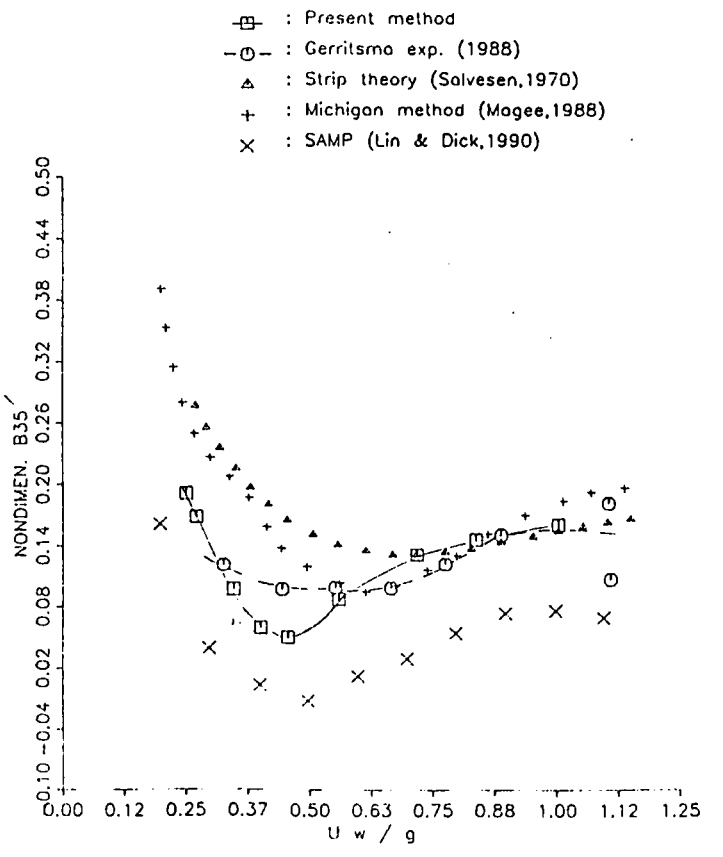

Fig. 9 Nondimensional B'_{35} of Wigley model

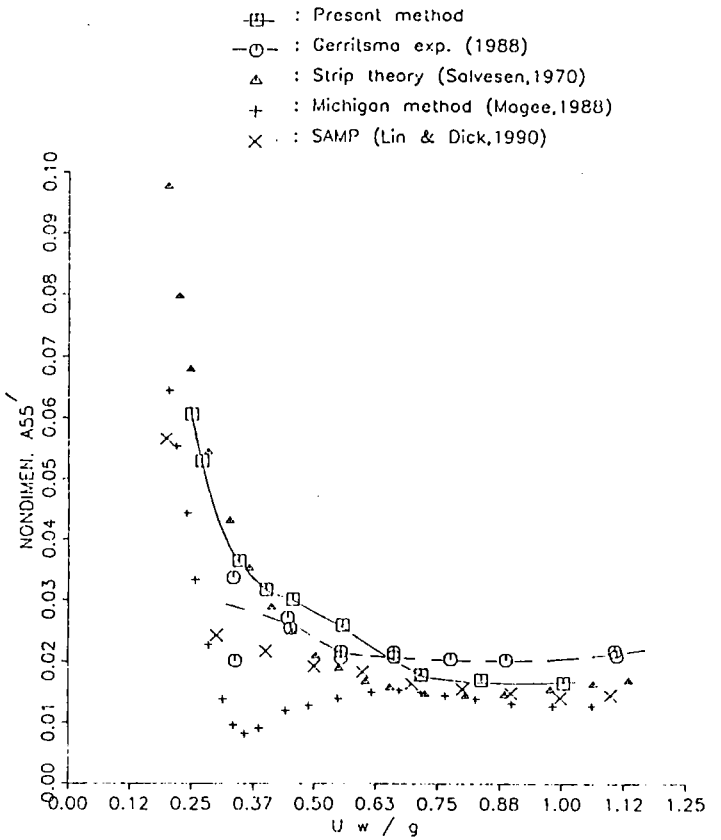

Fig. 10 Nondimensional A'_{55} of Wigley model

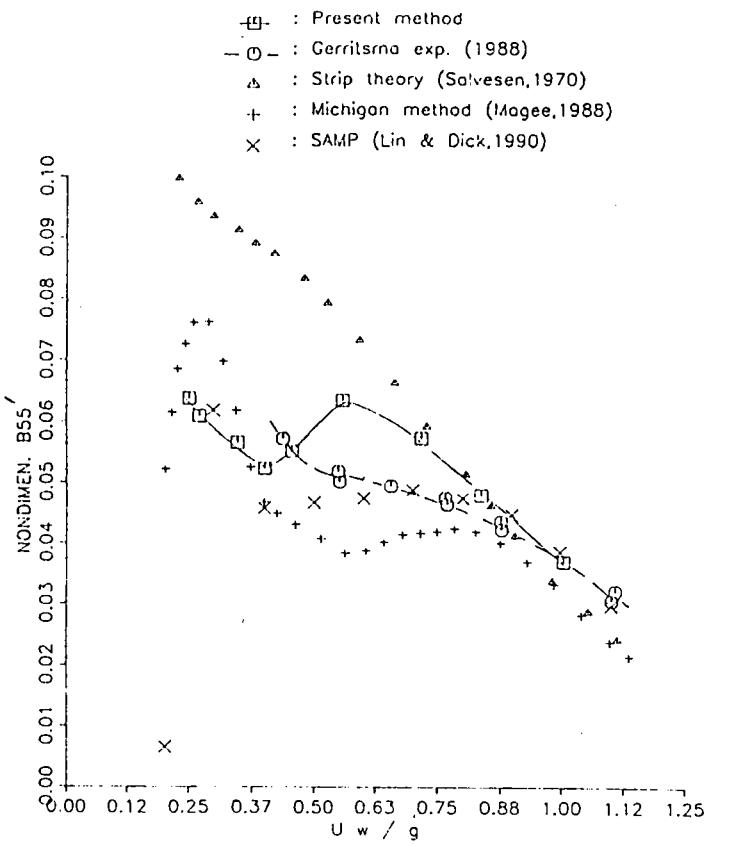

Fig. 11 Nondimensional B'_{55} of Wigley model

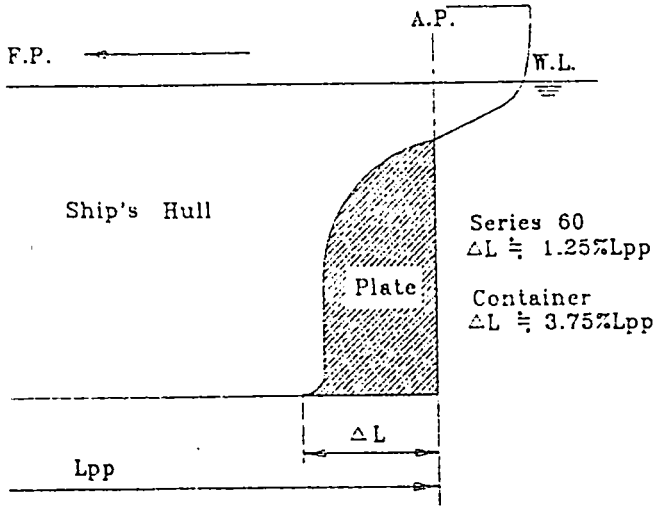

Fig. 12 Hypothetical dead wood behind the stern frame

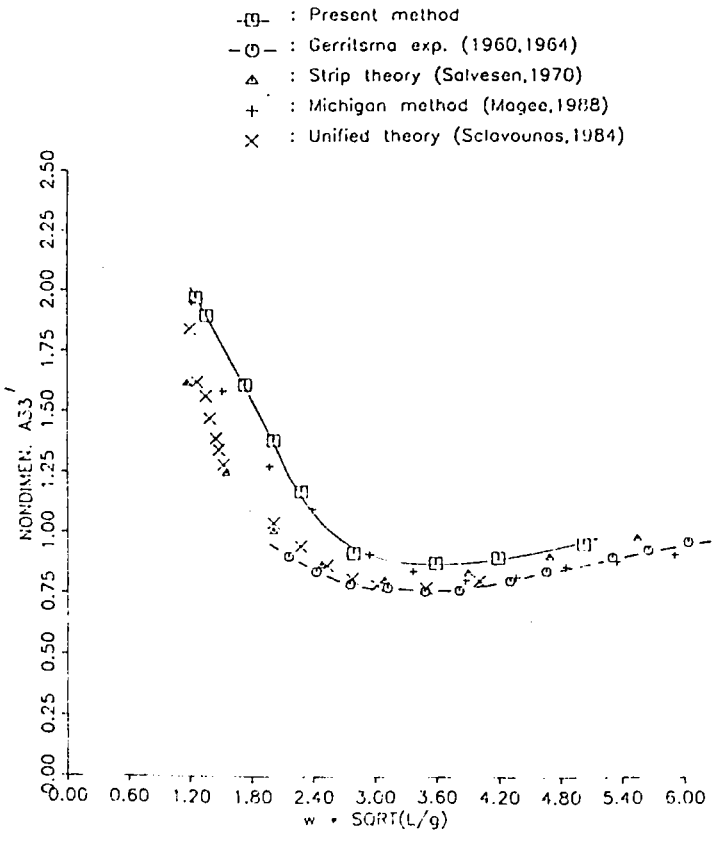

Fig. 13 Nondimensional A'_{33} of Series 60 model

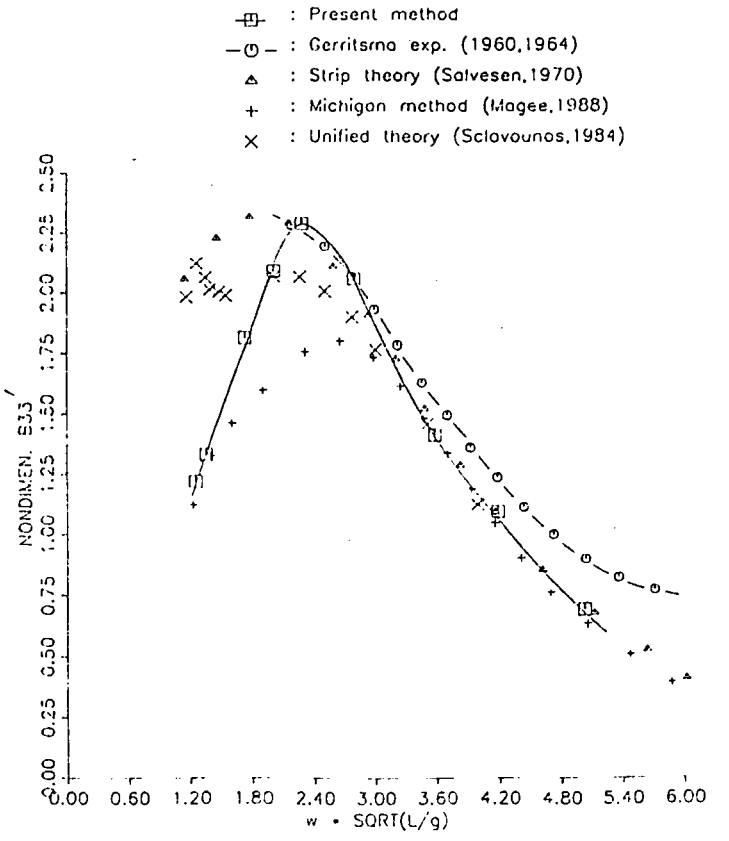

Fig. 14 Nondimensional B'_{33} of Series 60 model

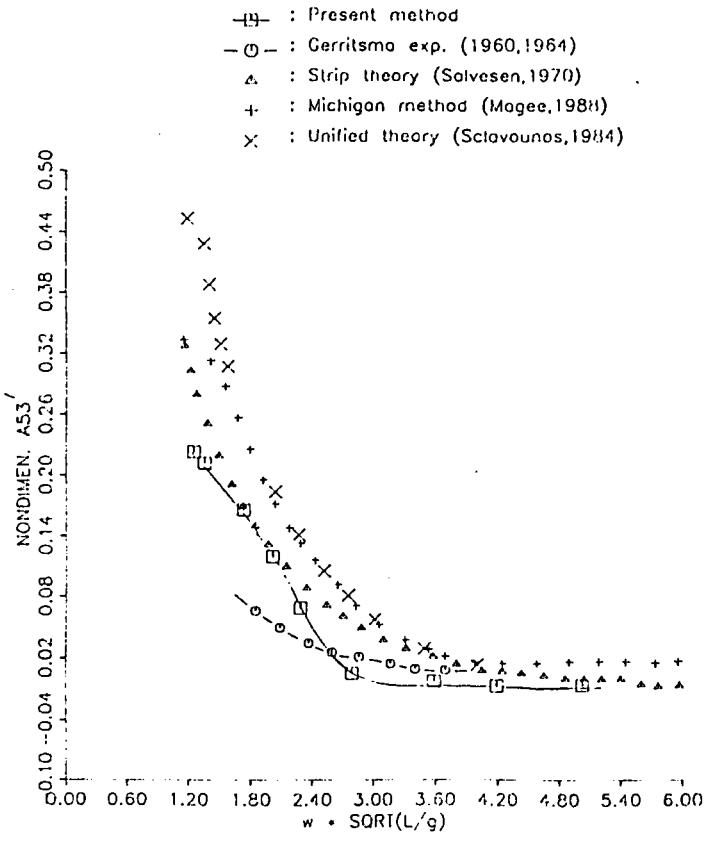

Fig. 15 Nondimensional A'_{53} of Series 60 model

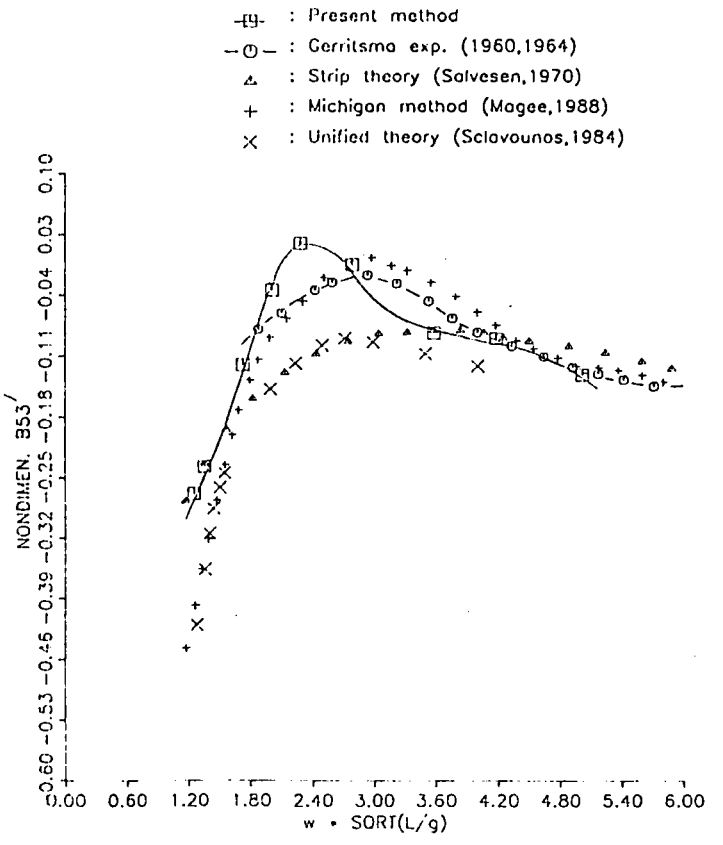

Fig. 16 Nondimensional B'_{53} of Series 60 model

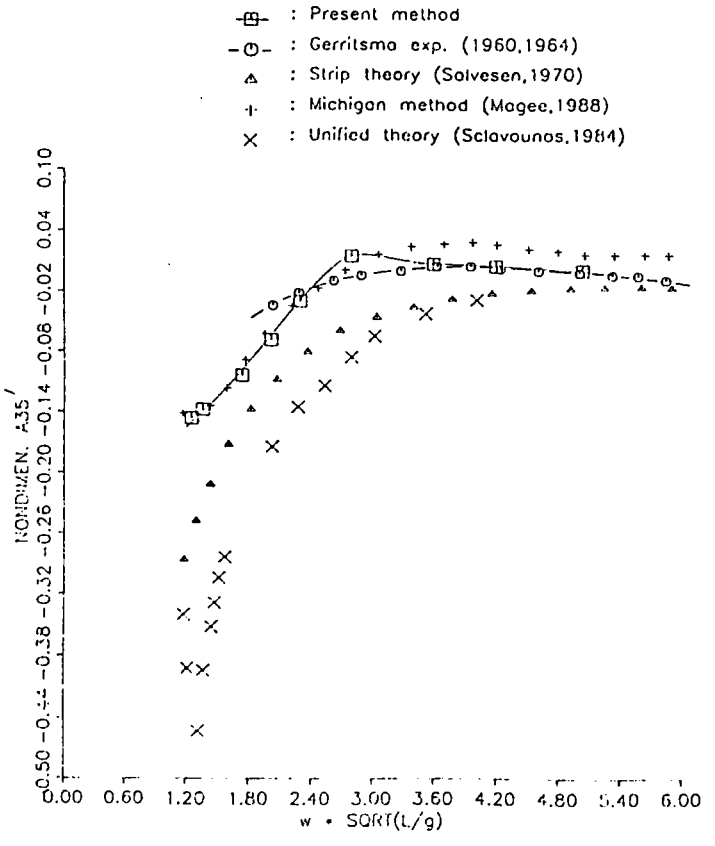

Fig. 17 Nondimensional A'_{35} of Series 60 model

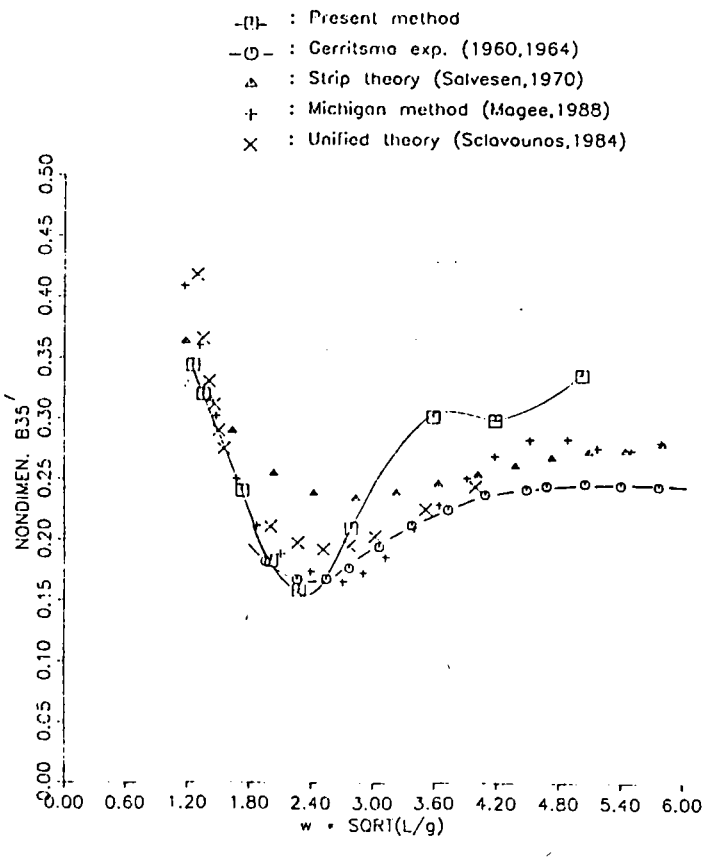

Fig. 18 Nondimensional B'_{35} of Series 60 model

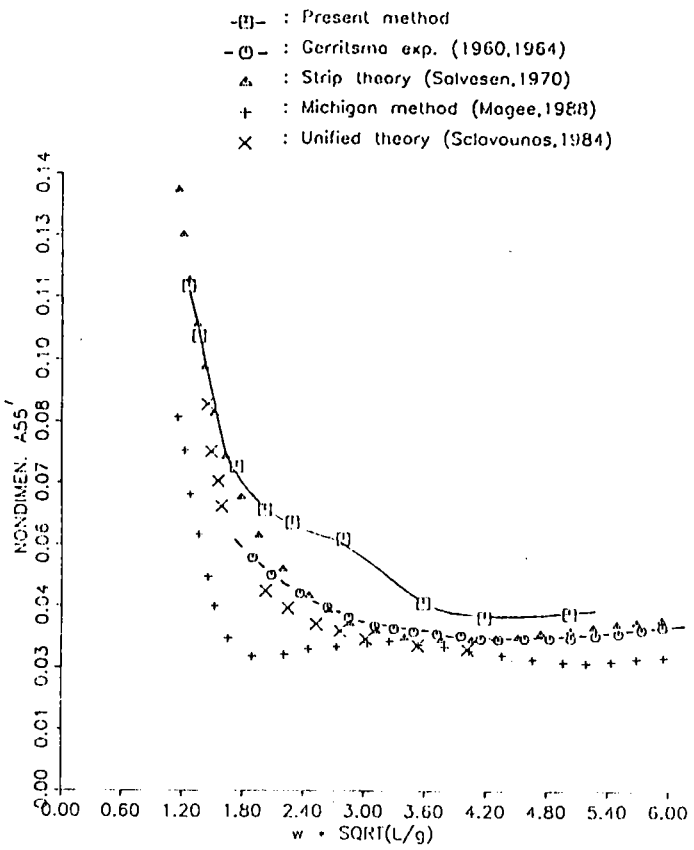

Fig. 19 Nondimensional A'_{55} of Series 60 model

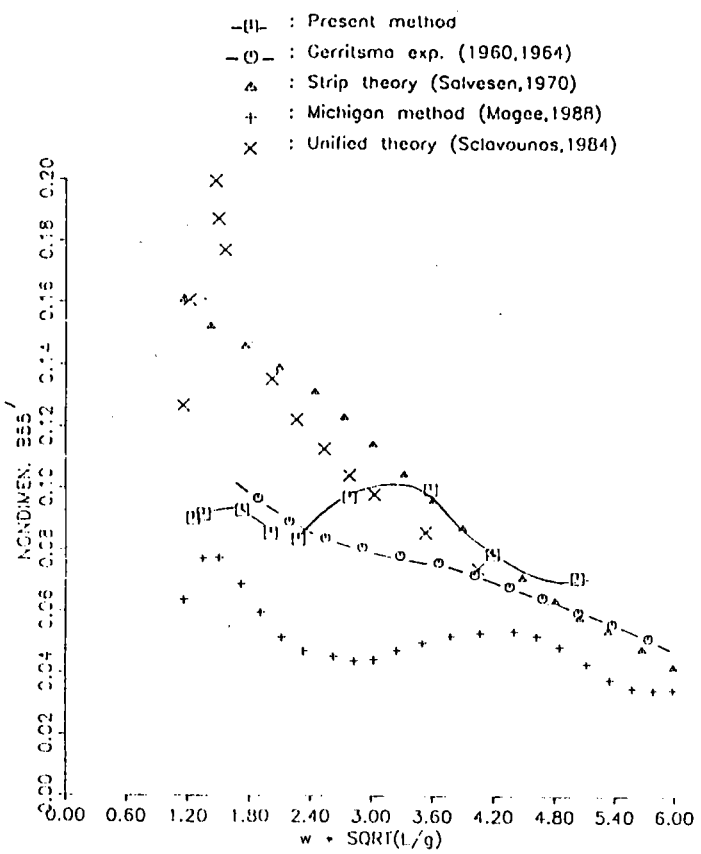

Fig. 20 Nondimensional B'_{55} of Series 60 model